Milky Way's Supermassive Black Hole: Recent Injuries To The Galaxy

Author's Student Number: 219046104[1]
Supervisor: Prof. Sergei Nayakshin[2,]

Department of Physics and Astronomy, University of Leicester

April 8, 2024

ABSTRACT

Context. To investigate the physical nature of Fermi Bubble in the ISM, the non hydro-dynamical simulations of the supernovae expansion used to model Fermi Bubbles, optically thin sphere filled of interstellar gas is analysed on the basis of supernovae shock model.
Massive Giant Molecular Clouds (GMC) deposited in the inner center of the Galaxy explain the origin of unusually massive young stars that are born there about 6 MYr. An unknown fraction of this gas is assumed to be accreted by Sgr A^*, the supermassive black hole (SMBH) in the center of the Galaxy.
Recently suggested that two observed γ-rays emitting bubbles emerging from from the very center of our galaxy, inflated by this presumed activity of Sgr A^*.
Aims. We aim to reconstruct models of different phases of supernovae remnant (SNR) using analytical and numerical solution and by understanding the nature and activity happening in the inner parsec of the centre of the Milky Way Galaxy, use these models to simulate the behaviour of Fermi Bubbles with changed density parameters.
Methods. The equations calculated for the expansion of a supernovae shell displayed for three separate phase i.e. Free Expansion, Energy Conserving and Momentum Conserving phase. These displays may be used to determine the behaviour of the Fermi Bubbles expanding from the centre of the Milky Way's Supermassive Black Hole by directly analysing the equations for the different phases of the expansion, specified by quantities such as density ρ, radius R, Energy of the supernovae E_{SN}, elapsed time t, velocity of the ejected material v_e. Instabilities may present in the (v_e, t) plane which would be described in this paper.
Results. It was found that for the free-expansion phase of the supernovae, the supernovae expands at a constant velocity due to initial blast and no hindrance from the ISM. For the adiabatic phase, the solution becomes a power-law and the the shell starts to decelerate due to ISM around the shell slowing it down. Using these models for Fermi bubbles, the radial change with time was found to be self-similar behaviour. The energy of the Fermi bubble was found to be continuously growing instead of being constant due to constant accretion of the Sgr A^*.
Conclusions. It was concluded that by comparing the radial expansion with respect to time shown in the graphs that the equations used to model different phases of supernovae remnant can be used to model the Fermi Bubbles with some parameters changed.

Key words. Fermi bubbles – ISM – supernovae remnant – expansion phases –

1. Introduction

Supermassive black holes, such as Sagittarius A* (Sgr A*) at the heart of the Milky Way Galaxy, wield noteworthy influence over the dynamics of their host galaxies. Recent studies have unveiled not only the profound gravitational effects of Sgr A* but also the intriguing phenomena known as the Fermi bubbles, further adding to the complexity of the galactic environment.

Alongside the enigmatic presence of Sgr A*, the Milky Way hosts the remarkable Fermi bubbles, expansive formations spanning thousands of light-years bilaterally and almost symmetrically from the centre of the galactic plane. These intriguing features were initially identified using gamma-ray observations from the Fermi Gamma-ray Space Telescope. Despite considerable scientific inquiry, the origins and significance of the Fermi bubbles remain subjects of ongoing investigation, mirroring the enigmatic nature of Sgr A* itself.

1.1. Evidence for Sgr A^*

The examination of stellar orbits within the Galactic Center has played a pivotal role in determining both the mass and distance to the central supermassive black hole. Through a meticulous analysis of star trajectories, researchers have approximated the mass of the black hole to be approximately 4.4 million times that of the Sun, with its position aligning closely with the radio source known as Sgr A* (Genzel et al. 2010; Ghez et al. 2008). This analysis entailed the fitting of orbital data, rigorous testing of the central mass's location, and careful consideration of

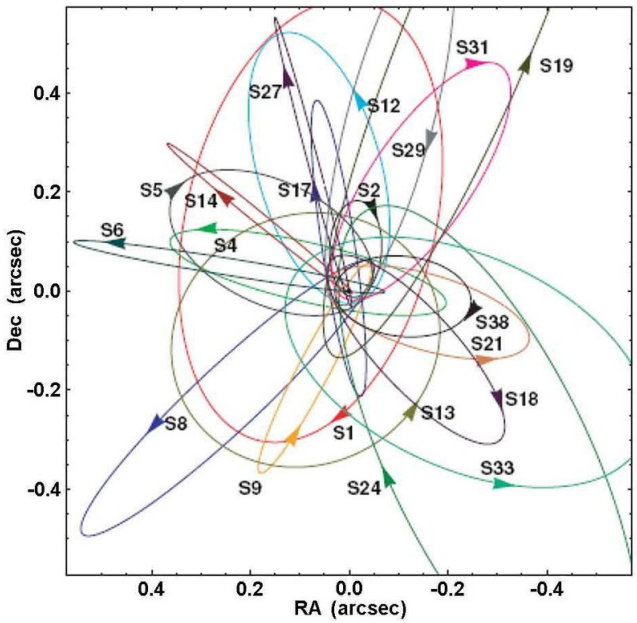

Fig. 1: (left) Orbits of individual stars near the Galactic centre. (right) The orbit of star S2 (black trajectory) around the SMBH and associated radio source Sgr A * based on observations of its position from 1992 to 2012. Results from the Ghez group (Ghez et al. 2008) using the Keck telescope and from the Genzel group (Genzel et al. 2010) using the European Very Large Telescope (VLT) are combined.

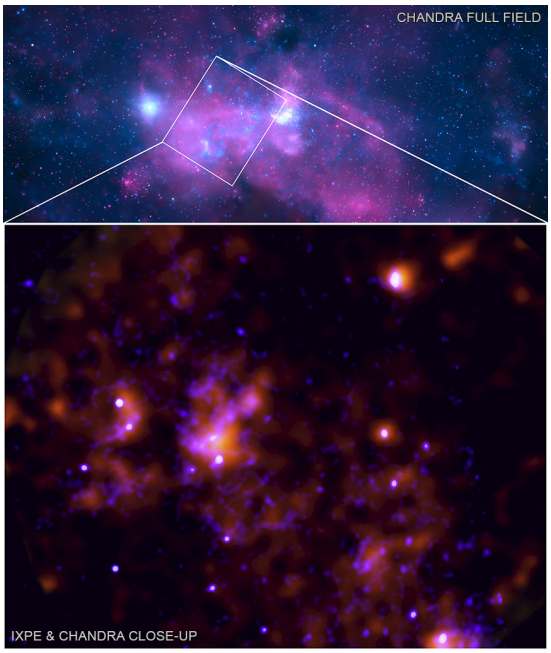

Fig. 2: NASA's IXPE reveals intense activity in Sagittarius A*, the supermassive black hole at the Milky Way's core, some 200 years ago. Echoes of this event (orange) are seen alongside direct light captured by Chandra (blue), offering insight into past cosmic activity.

potential systematic errors and parameter correlations.

Moreover, the study underscored the significance of precise measurements and highlighted the potential influence of systematic uncertainties on the outcomes. Additionally, investigations into the historical activity of Sgr A* have yielded valuable insights into its past behavior. Potential explanations explored include the accretion of colliding stellar winds, tidal disruptions of stars, and interactions with other X-ray sources (Ghez et al. 2008; Genzel et al. 2010).

Sgr A^* is known to be extremely faint, with it's bolometric luminosity measured to be $L_b = 10^{43} Js^{-1} = 2 \times 10^{-9} L_{Edd}$ i.e. 9 orders of magnitude lower than the Eddington luminosity for the mass of the black hole $M_{BH} = 3.6 \sim 4.4 \times 10^6 M_\odot$ (Ghez et al. 2008; Gillessen et al. 2009)

A recent groundbreaking study, led by Frédéric Marin and a team of international scientists from the Astronomical Strasbourg Observatory, has illuminated a previously unknown aspect of the behaviour of Sagittarius A* (Sgr A*), the supermassive black hole nestled at the heart of our Milky Way galaxy. Published in the prestigious journal Nature, the research unveils a fascinating revelation: approximately two centuries ago, Sgr A* underwent a dramatic shift from a long period of dormancy to a brief phase of heightened activity (Marin et al. 2023).

This revelation marks a significant milestone in our understanding of the dynamic behaviour of supermassive black holes, particularly those residing in the centres of galaxies. Sagittarius A*, with its staggering mass of four million times that of our Sun, has long been a subject of intense scrutiny and fascination among astronomers and astrophysicists alike. Yet, until now, the specifics of its past activity remained shrouded in mystery.

During the one-year window of heightened activity, Sgr A* exhibited a voracious appetite, devouring cosmic objects that strayed too close to its gravitational grasp. However, despite this cosmic feast, Earth remained blissfully unaffected, as the immense distance between our planet and Sgr A* (approximately 2 billion times the distance from Earth to the Sun) served as a formidable barrier against any potential repercussions.

The most intriguing aspect of this study lies in the detection of an X-ray echo emitted approximately two centuries ago, during Sgr A*'s brief moment of activity. This echo, captured by NASA's IXPE (Imaging X-ray Polarimetry Explorer) satellite, provides compelling evidence of the black hole's past behaviour. Surprisingly, the intensity of the X-ray emission during this period was estimated to be at least a million times greater than its current emissions—a revelation that astounds and captivates scientists.

1.2. Past Activity of Sgr A^*

The historical behavior of the supermassive black hole Sgr A* positioned at the heart of our galaxy has been a focal point of inquiry aimed at comprehending its past dynamics. Recent investigations propose that Sgr A* might have undergone notable episodes of X-ray emissions in earlier epochs, potentially surpassing luminosities several

magnitudes brighter than contemporary observations indicate (Ponti et al. 2010). Notably, evidence gleaned from X-ray emission patterns in the surrounding interstellar medium points to a significant X-ray outburst occurring roughly 300 years ago, hinting at a phase of heightened activity (Ponti et al. 2010).

Observations reveal that Sgr A* predominantly maintains a quiescent state, punctuated by sporadic flares that can attain luminosities of up to 10^{35} erg s^{-1}. Nonetheless, clues of past outbursts and interactions with sizable molecular clouds in the vicinity offer glimpses into the historical luminosity variations of the black hole over the last six to nine decades (Cramphorn and Sunyaev 2002).

Efforts have been made to gauge the likelihood of detecting past Sgr A* flares based on their duration and luminosity. Studies indicate that detecting an Eddington level flare persisting longer than approximately 300 years within the last 40,000 years is improbable, with flares surpassing 3000 years deemed unlikely based on existing data (Cramphorn and Sunyaev 2002).. By analyzing scattered flux and mass distribution in the interstellar medium, researchers have established constraints on the historical X-ray activity of Sgr A*, excluding certain luminosity levels for past events (Cramphorn and Sunyaev 2002).

Moreover, investigations into the evolution of X-ray emission regions encircling Sgr A* unveil causal disconnections between emitting areas. Despite significant spatial separations on the celestial sphere, intensity rises in distinct regions exhibit delays of 2-4 years, suggesting a nuanced and dynamic history of X-ray activity in Sgr A*'s vicinity (Ponti et al. 2010).

1.3. Feedback from the SMBH

The emergence of a quasi-spherical cluster of young stars within the central parsec of the Milky Way is intricately linked to the star formation induced by active galactic nucleus (AGN) feedback. This population of young stars is believed to have originated from the fragmentation of a substantial quasi-spherical gas shell, propelled outward and compressed by the feedback mechanisms of Sgr A* (Nayakshin and Zubovas 2018).

According to this scenario, these stars are hypothesized to have formed from atomic hydrogen subjected to immense pressure exerted by outflows from the black hole. Notably, the distinguishing factor between the quasi-spherical population of young stars and the disk stars within the same region lies in their respective formation processes and characteristics (Nayakshin and Zubovas 2018).

The disk stars originate from the gravitational collapse of a massive gaseous disk, a process which typically inhibits fragmentation within a radius of approximately 0.03 parsecs. In contrast, the quasi-spherical cluster of young stars undergoes a distinct formation process, involving the fragmentation of a substantial gas shell propelled outward by AGN feedback. Consequently, these stars exhibit randomly oriented orbits with larger semi-major axes (Nayakshin and Zubovas 2018).

Moreover, while the quasi-spherical population of young stars forms from atomic hydrogen, the disk stars primarily originate from molecular hydrogen. This differentiation underscores the diverse origins and characteristics of stellar populations within the central parsec of the Milky Way (Nayakshin and Zubovas 2018).

1.4. Fermi Bubbles: A Result from AGN Feedback?

Recent investigations have unveiled a dynamic interplay between Sgr A* and the Fermi bubbles. *Fermi*-LAT data divulged two giant γ-ray emitting bubbles, inclined symmetrically on both sides of the Galactic plane, with the gravitational influence of the supermassive black hole potentially shaping the formation and evolution of these colossal structures (Su and others. 2010). Moreover, the interaction between Sgr A* and the Fermi bubbles may offer crucial insights into the broader processes governing galactic dynamics and the co-evolution of supermassive black holes and their host galaxies.

The investigation initiates with a systemic study of the distinct stages that characterize supernova explosions. Beginning with the Sedov-Taylor phase, which is notable for its adiabatic expansion and propagation of shock waves, a fundamental comprehension of the mid-stage evolution of supernova remnants is established. Following this, the focus is directed towards modelling the free expansion phase, the first and a very crucial stage where remnants of supernova experience unhindered expansion into the interstellar medium. A deeper understanding of the chronological evolution of supernova remnants is attained through meticulous simulation of the interactions between these phases and identification of transition points. This understanding extends from the initial detonation to subsequent deceleration and interactions with the surrounding medium.

With refined models of supernova evolution in hand, focus turns to the enigmatic Fermi bubbles—expansive structures extending both above and below the galactic plane. Leveraging insights gleaned from supernova modeling efforts, parameters are rigorously adjusted to align with observed characteristics of the Fermi bubbles. Through meticulous numerical manipulations using Python, efforts are made to unveil potential correlations between these colossal structures and the dynamic interplay of supernova remnants within the galactic environment.

The methodology integrates advanced numerical techniques with robust astrophysical theory, providing a rigorous framework to investigate the relationship between supernova evolution and the mysterious Fermi bubbles. Through unraveling the intricacies of these phenomena, significant strides are made towards enhancing our comprehension of galactic dynamics and the overarching processes that govern the universe.

2. Three Stages of Supernovae Remnant

In this section, the three phases of the supernovae explosion along with the numerical and analytical methods used to

model the said phases will be discussed. The consequences of the supernovae explosion result in supernovae remnants which are the main sources of heating of the interstellar gas (Mathis 2024).

Supernovae possess immense power, generating new atomic nuclei through a remarkable process. When a massive star undergoes collapse, it generates a shock-wave capable of initiating fusion reactions within its outer shell. This fusion process, known as nucleosynthesis, results in the creation of new atomic nuclei. Supernovae are recognised as one of the primary sources responsible for the existence of elements heavier than iron in the Universe. After a core collapse supernova, all that remains is a dense core and hot gas shell called a nebula. When stars are especially large, the core collapses into a black hole. Otherwise, the core becomes an ultra-dense neutron star.

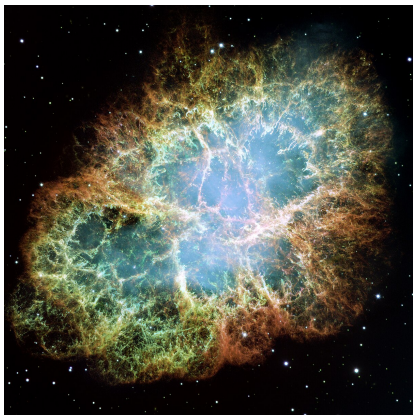

Fig. 3: Crab Nebula: an SNR in it's early stage, with the central compact object being a rapidly spinning neutron star

In a supernovae explosion, a forward and reverse shock are created when the supernovae wave interacts with ISM (Inter-Stellar Medium). The forward shock continues to expand into the ISM, the reverse shock travels back into the freely expanding supernovae ejecta.

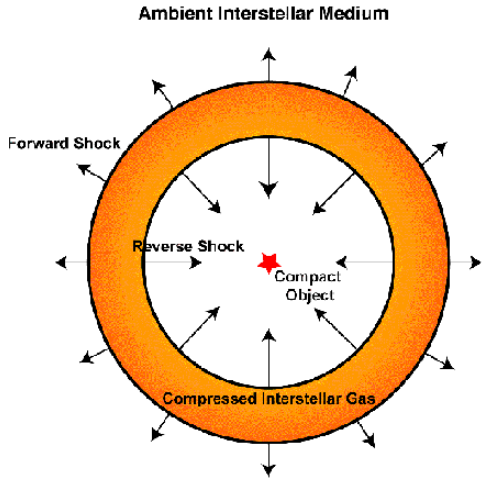

Fig. 4: Shell of compressed ISM material and stellar ejecta

The evolution of these remnants unfolds through a series of distinct phases, each characterized by unique physical processes and observable phenomena. The three primary phases of supernova remnant evolution: the free expansion phase, the Energy-Conserving (Sedov-Taylor) phase, and the Momentum-Conserving (snow plow) phase delineate the journey of supernova debris as it expands into the interstellar medium, encountering varying degrees of resistance and undergoing complex interactions that shape its structure and dynamics. By understanding the progression through these phases, we gain valuable insights into the aftermath of supernova explosions and the dynamic interplay between stellar remnants and their surrounding environments but also shedding light on broader galactic phenomena such as the Fermi bubbles.

2.1. Phase 1. Free Expansion Phase

During this phase, interstellar gaseous matter moves outward very fast with about a constant velocity of $v_{ejecta} = 10,000 kms^{-1}$ into the interstellar medium. These emission have been ejected from the center of the star, where nucleosynthesis takes place.
During this phase, the outer layers of the star i.e the interstellar gaseous matter, previously held in place by the star's gravity, are ejected into the surrounding interstellar medium at an extraordinary velocity which remains constant (about $v_{ejecta} = 10,000 kms^{-1}$). This expulsion of material occurs with little resistance, as the outward force generated by the explosive energy overwhelms the gravitational pull of the remnants left behind. As a result, the expanding shell of debris expands freely into the interstellar medium, carrying with it the heavy elements synthesized during the star's lifetime. The free expansion phase marks the initial stage of the supernova's evolution, setting the stage for subsequent interactions with its surroundings and leaving an indelible imprint on the galactic environment.

2.1.1. Mathematical Modelling

The ejection velocity for the material can be estimated using the simple kinetic energy equation

$$K.E. = \tfrac{1}{2} M_e v_e^2 \tag{1}$$

Assuming most of the supernovae energy is transformed into kinetic energy:

$$E_{SN} = \tfrac{1}{2} M_e v_e^2 \tag{2}$$

re-arranging this for the ejecta velocity:

$$v_e = \sqrt{\tfrac{2E_{SN}}{M_e}} \tag{3}$$

where energy of the supernovae, $E_{SN} = 10^{44}$ J.
The relation between velocity and radius can be given by $R_s(t) = \boldsymbol{v_e} t$ which can then be used to form a graphical representation of the said model.
One notable characteristic of the free expansion phase is the linear relationship between the remnant's radius and

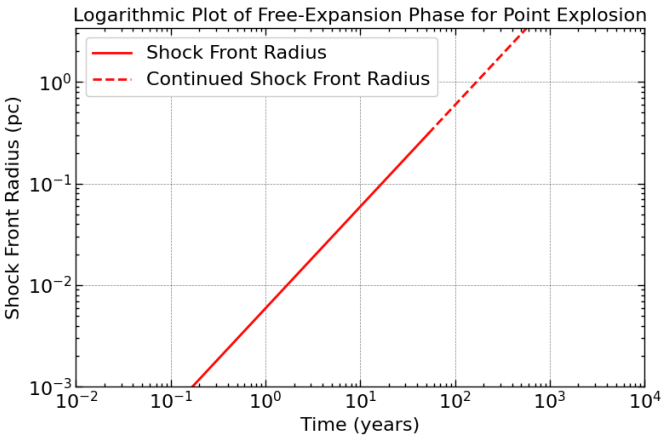

Fig. 5: Free Expansion Phase, radial change with time

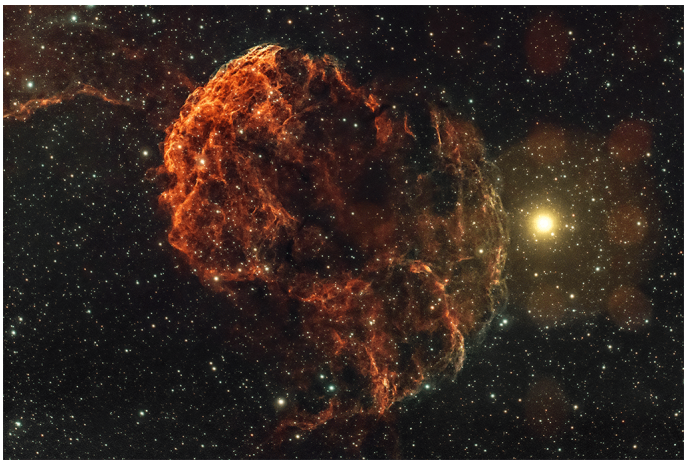

Fig. 6: IC 443, The Jellyfish Nebula believed to be in Adiabatic Phase

the time elapsed since the supernova explosion. This linearity arises from the uniform expansion of the ejecta into the surrounding space, with the radius increasing at a constant rate over time. This constant rate of expansion indicates that the shell expands at a constant velocity throughout the free expansion phase. As a result, when plotted on a graph, the radius versus time curve exhibits a straight-line behavior, reflecting the consistent expansion of the remnant during this phase.

2.2. Phase 2. Adiabatic Conserving (Sedov-Taylor) Phase

In the Sedov-Taylor phase, the supernova remnant transitions from the initial free expansion phase to a phase of deceleration as it encounters the surrounding interstellar medium which puts a hindrance in its expansion. The expanding shock wave begins to sweep up and compress the ambient gas, forming a dense shell of shocked material around the remnant.

The remnants found in the Sedov-Taylor expansion expansion phase refer to the supernovae remnants (SNRs) that are expanding adiabatically into a uniform ambient medium . The Sedov-Taylor model is used to describe is employed to characterise this phase of the SNR evolution, where the initial energy of the supernovae blast, the density of the ambient medium, and the duration following the detonation of the supernovae are the governing parameters. The shocked interstellar medium (ISM) is the focus of the Sedov-Taylor model, with the mass of the shocked interstellar medium (ISM) surpassing that of the material expelled by the supernova. This phase typically last for tens of thousands of year after the free expansion phase (Borkowski et al. 2001)

Figure 6 shows the Jellyfish Nebula (IC 443) believed to be result of supernovae explosion, which is estimated to have happened between 3,000 years ago. The dark lane crossing the SNR in the middle is not due to the separation of the shell into two parts, but rather a giant molecular cloud (GMC) in between the remnant and the observer, which obstructs the view.

The Sedov-Taylor solution serves as a theoretical framework that elucidates the progression of supernova remnants during this particular phase. It provides valuable insights into various aspects such as the propagation of shock-waves, the deposition of energy, and the emission of thermal radiation. Originating independently by Sedov and Taylor in the 1940s, notably during the Second World War for the Trinity explosion, this solution has evolved into a cornerstone of astrophysical research. Its application extends to facilitating the interpretation of observational data and the modelling of supernova remnant evolution across a wide array of astrophysical contexts.

Leonid Sedov, Geoffrey I. Taylor and John Von Neumann worked on this solution originally for the trinity explosion, which was the first nuclear fission explosion tested in Los Alamos during the second world war. The nature of expansion of the blast radius with respect to time are similar to that of a supernovae explosion which is why the said solution's used for the energy-conserving phase of the supernovae explosion.

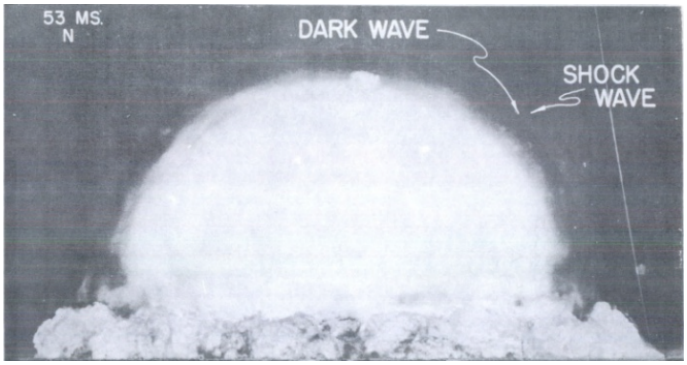

Fig. 7: Trinity Test Fireball
(Mack and Ellis 1946)

2.2.1. Modelling Adiabatic Phase

Modeling the Sedov-Taylor phase in supernovae is critical in understanding the aftermath of these cataclysmic events.

One approach to modeling the Sedov-Taylor phase involves employing analytical methods. The Sedov-Taylor solution provides mathematical expressions derived from fundamental physical principles to depict the evolution of supernova remnants during this phase. These analytical models offer valuable insights into various aspects such as shock-wave propagation, energy deposition, and radial expansion. By solving equations derived from conservation laws and employing idealized assumptions, a deeper understanding of the underlying physics governing supernova evolution can be attained.

In addition to analytical modeling, numerical techniques are integral for simulating the Sedov-Taylor phase. Numerical simulations entail discretizing the equations that govern supernova evolution and employing computational methods to solve them. This approach enables the depiction of complex interactions among diverse physical processes and facilitates the generation of detailed maps depicting physical quantities like density, temperature, and velocity within the supernova remnant. Numerical simulations serve as a potent tool for investigating the behavior of supernovae across diverse conditions and exploring the impact of varying parameters on their evolution.

2.2.2. Analytical Solution

To start with the modelling of the analytical solution to the adiabatic phase of the supernovae, a few assumption were considered:

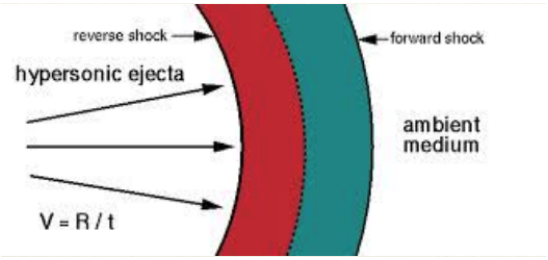

Fig. 8: Shock and Ejecta Dynamics for the Supernovae Shell

1. Mass of the SNR is dominated by the swept-up ISM (the green bubble)
2. Energy is dominated by the hot bubble i.e. $E_{bubble} = E_{SN}$, and therefore
3. Radiation is negligible

Mass of the swept-up shell can be described as:

$$M_{SW} = \frac{4\pi R_{SW}^3}{3}\rho_0 \tag{4}$$

Where ρ_0 is the density of the ambient medium $= 10^9$ Hydrogen molecules m^{-3}

Therefore, an equation for the momentum of the eject can be formed using the mass equation

$$\Pi_{SW} = M_{SW} v_{SW} = M_{SW}\dot{R}_{SW} \tag{5}$$

The force acting on the ejecta can be described as

$$F = \frac{d\Pi_{SW}}{dt} = P_{bubble} \times V_{SW} \tag{6}$$

Therefore, from equation 6

$$\frac{d\Pi_{SW}}{dt} = P_{bubble} \times 4\pi R_{SW}^2 \tag{7}$$

From the ideal gas law

$$P_{bubble} = nK_BT \tag{8}$$

and internal energy of the supernovae gas is given by the equation

$$\frac{3}{2}nK_BT = \frac{3}{2}NVK_BT \tag{9}$$

Therefore from equation 8 and 9,

$$P_{bubble} = \frac{2}{3}\frac{E_{SN}}{V} \tag{10}$$

Finally, the force equation can be written as

$$\frac{d\Pi_{SW}}{dt} = 4\pi R_{SW}^2 \times \frac{2}{3}\frac{E_{SN}}{V} \tag{11}$$

Now everything is in terms of R_{SW} and the equation can now be solved.

In order to solve the ordinary differential equation, a power-law solution of the form $R = At^{\eta}$ needs to be assumed.

After solving the O.D.E. (see derivation 5, the solution derived is

$$\eta = \frac{2}{5} \text{ and } A = \left(\frac{25E_{SN}}{4\pi\rho_0}\right)^{\frac{1}{5}}$$

Therefore, the equation for the radius expansion with time is given by

$$R_{SW} = \left(\frac{25E_{SN}}{4\pi\rho_0}\right)^{\frac{1}{5}} t^{\frac{2}{5}}$$

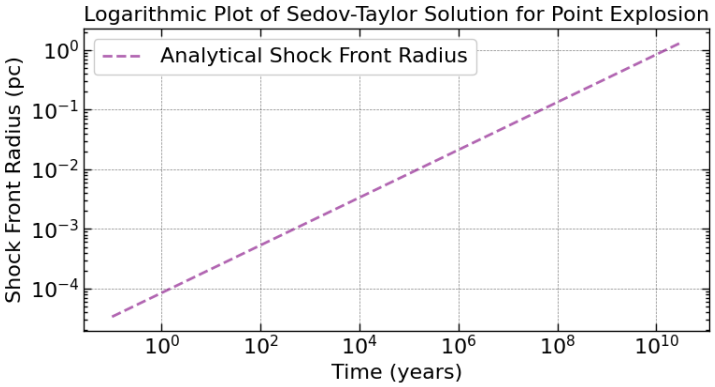

Fig. 9: Graphical Representation of Analytical Solution for Sedov-Taylor Phase of Supernovae Explosion

Equation 2.2.2 can now be used to fabricate a graphical representation of the radial expansion of supernovae with respect to time in this phase.

From the graphical representation, When plotted on a logarithmic scale, the Sedov-Taylor solution often manifests as a straight line—a characteristic feature indicative of self-consistent expansion therefore confirming the solution being a power law. This self-similarity arises from the conservation laws governing the dynamics of the expanding shock-wave, allowing for the scaling of physical quantities over time.

Interestingly, a similar logarithmic plot can be observed in the analysis of the Trinity test, the first detonation of a nuclear weapon conducted on July 16, 1945, in New Mexico, USA. In this case, the logarithmic plot typically depicts the evolution of the blast wave and its interaction with the surrounding atmosphere(Díaz 2021). Similar to the Sedov-Taylor solution, the Trinity test exhibits self-similar behaviour, with certain physical quantities scaling logarithmically over time.

To corroborate the generated analytical results for the Sedov-Taylor phase for the supernovae, the data from the infamous Trinity explosion replicated in paper by Jorge S. D´ıaz can be referred to to check if it matches the plot for the supernovae point explosion.

Comparing both the graphs, it can be seen that the derived mathematical expression matches the theory.

2.2.3. Numerical Solution

Despite having access to an analytical solution, the utilization of a numerical approach becomes imperative. This allows us to thoroughly assess the precision and fidelity with which a methodical procedure can replicate the expected outcomes. The numerical representation, if accurate enough tells us the same thing visually as the analytical model which is what tells if the methods are accurate. Numerical approaches also gets the advantages due to its nature of being repetitive to solve complex problems like such that require a lot of iterations.

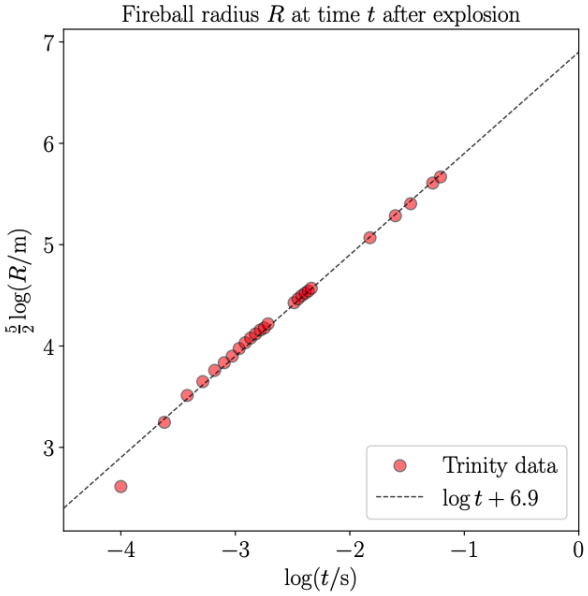

Fig. 10: Graphical Representation of Radial Change of Trinity Shell with Respect to Time (Díaz 2021)

A numerical solution to Sedov-Taylor phase, akin to approach utilised for the free-expansion phase is implemented by initialising arrays with zero values and employing time integration techniques. This methodology enables the numerical simulation to evolve over successive time steps, capturing the dynamic evolution of the explosion according to the Sedov-Taylor model.

During the numerical simulation, the Sedov-Taylor equations are discretised and solved iteratively using numerical methods such as finite difference or finite volume techniques. At each time step, the values of physical quantities are updated based on the calculated changes and boundary conditions, allowing for a comprehensive analysis of the explosion dynamics.

Once the numerical simulation is completed, a graphical representation of the results is generated to visually depict the evolution of the explosion. This graphical representation typically includes plots of key parameters such as density, pressure, velocity, and shock front position as functions of time or spatial coordinates. These plots provide valuable insights into the behavior of the explosion and facilitate comparison with theoretical predictions.

From the graphical representation for both analytical and numerical solutions and on comparing, it can be visually seen that after a certain time period, both the solutions start matching up. The main reason of this is due to not considering the free-expansion phase for the numerical Sedov-Taylor solution, therefore showing a constant radius for a certain time period before switching up to adiabatic phase. This switch-over can be shown by combining both the free-expansion and Sedov-Taylor models in the same graph to understand at what time period does the switch-over takes place.

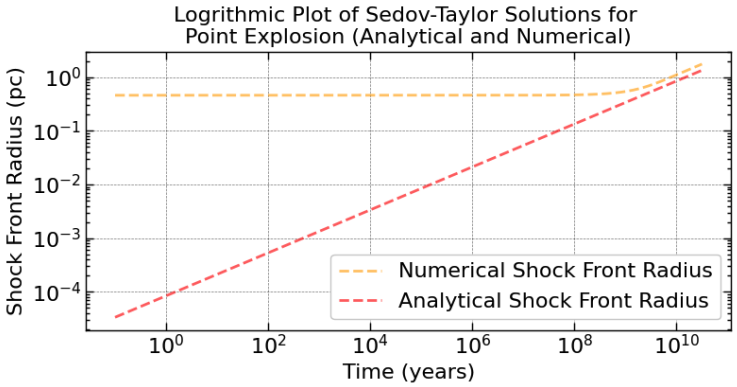

Fig. 11: Analytical and Numerical Solution for Sedov-Taylor phase

2.2.4. Phase Switch-Over

To examine the switch-over from free-expansion phase of the supernovae to adiabatic phase, the graphical representation of radial change with time can be combined together and by monitoring the radius and time using iterative loop method and when they are the same but change as a power law, then the switch-over can be made at that moment.

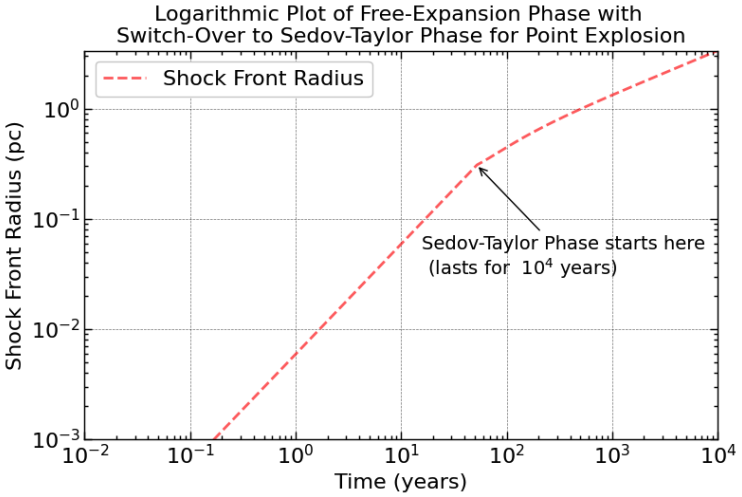

Fig. 12: Switch-Over from Free-Expansion Phase to Sedov-Taylor Phase

Upon analyzing the switch-over graph (see Figure 12), it becomes evident that the transition from the free-expansion phase to the Sedov-Taylor phase aligns closely with theoretical predictions. The cessation of the free-expansion phase at approximately 100-200 years concurs with expectations based on established models of supernova evolution. This critical juncture marks the point at which the initial energy released from the supernova dissipates, giving way to the onset of the Sedov-Taylor phase.

Furthermore, the prolonged duration of the Sedov-Taylor phase, enduring for about 10,000 years as depicted in the graph, mirrors the anticipated longevity posited by theoretical frameworks. This extended phase allows for the continued expansion of the supernova remnant, as the shock-wave interacts with the surrounding interstellar medium, driving its evolution over millennia.

Finally, a graph with the analytical solution overlapping the switch-over model can be shown to accurately examine if there's a close correspondence between the analytical solutions derived and the numerical methods used by us in the modelling of the different phases.

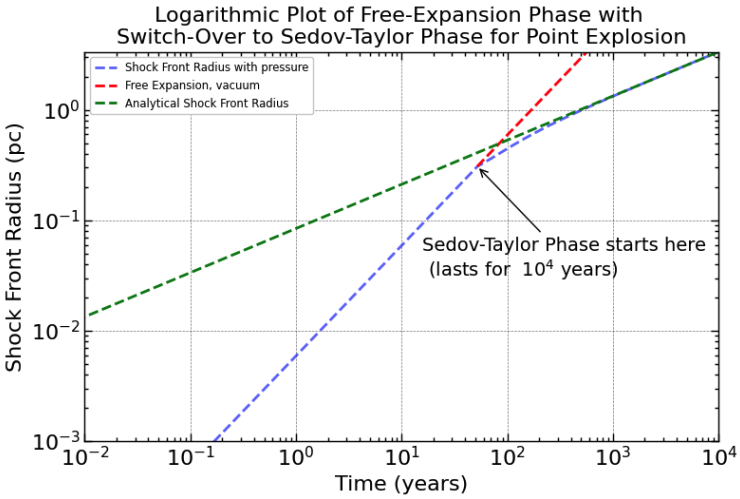

Fig. 13: Switch-Over from Free-Expansion Phase to Sedov-Taylor Phase

The close correspondence between the modelled switch-over times and theoretical expectations underscores the accuracy and efficacy of the numerical approach employed in our study.

2.3. Velocity Dynamics of Ejecta and Swept-Up Material

To gain insights into the velocity dynamics of both the ejecta and the swept-up material across various phases of the supernova event, it is essential to reexamine the graphs depicting radial changes over time.

2.3.1. Density as a Parameter

The density of the surrounding medium plays a pivotal role in shaping the evolution of supernova remnants, particularly during the transition to the radiative phase post-explosion. Notably, our observations underscore a compelling relationship between medium density and the timing of this critical transition, occurring approximately 1000 years after the initial explosion.

In regions characterized by higher medium densities, the transition to the radiative phase is notably delayed. Here, the shock front faces increased resistance from the denser medium, impeding energy dissipation and prolonging the remnant's evolution in the non-radiative phase. This delayed transition underscores the significant influence of medium density on the temporal dynamics of supernova remnants (Chiad et al. 2015).

A lower density environment facilitates an earlier entry of supernova remnants into the radiative phase. In such scenarios, the shock front encounters less resistance, allow-

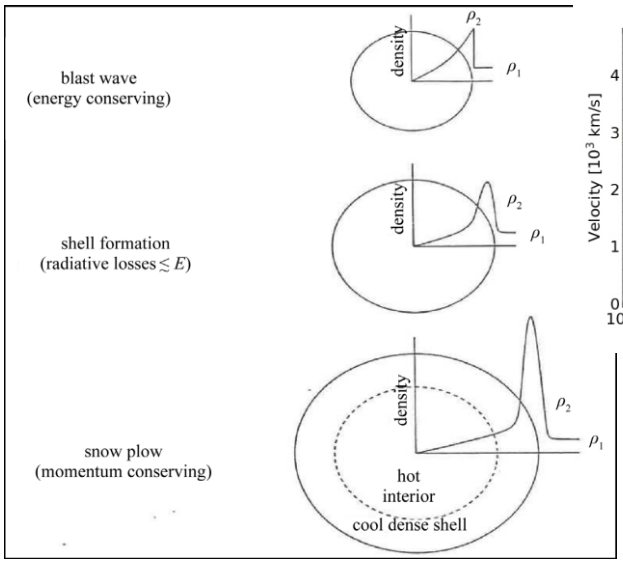

Fig. 14: Density Profile for Different Phases of Supernovae Explosion (Chiad et al. 2015)

ing for more efficient energy dissipation through radiation. Consequently, the transition to the radiative phase occurs sooner, marking the onset of a new phase in the remnant's evolution (Chiad et al. 2015).

2.3.2. Modelling Velocity Dynamics

Upon analyzing the graph depicted in Figure 5, it becomes evident that a linear relationship exists between the remnant's radius and the time elapsed since the supernova explosion. This linear trend arises from the uniform expansion of the ejecta into the surrounding space, resulting in a consistent increase in radius over time. Consequently, this observation suggests that the change in velocity with respect to time remains constant (i.e., constant velocity) throughout this phase of the supernova evolution.

Upon examination of the Sedov-Taylor graph depicted in Figure 11, a notable pattern emerges—a straight line. This linear correlation between radius and time signifies a self-similar expansion of the supernova remnant, characteristic of the Sedov-Taylor phase. However, as the interstellar medium begins to impede the expansion of the swept-up material, a gradual deceleration in the velocity of the ejecta is anticipated.
Using similar numerical methods used for free-expansion phase and adiabatic phase, the velocity dynamics can be modelled for the supernovae expansion.

Analysis of Figure 15 reveals distinct phases in the velocity profile of the ejected compressed interstellar gas. Initially, spanning approximately 100-200 years, the velocity remains relatively constant at a high magnitude, around ∼10,000 km/s. This phase bears striking resemblance to the free expansion phase of the explosion, characterized by rapid expansion of the ejecta.

Following this initial phase, a notable transition occurs, marked by a sudden increase in velocity followed by a gradual deceleration of the ejected material. This observed change is attributed to the interaction with the ambient

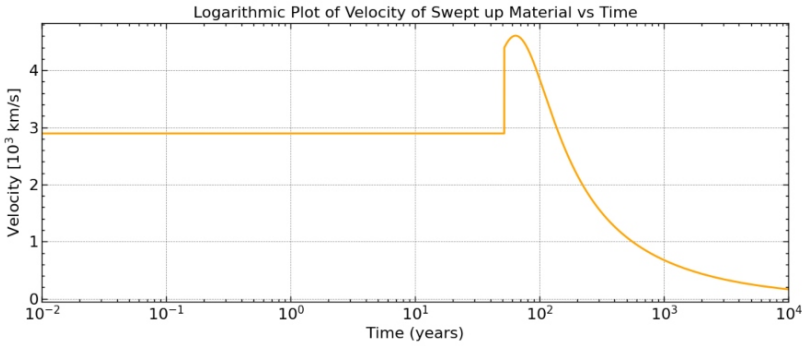

Fig. 15: Log Plot of Velocity of the Ejecta with Time Span

interstellar medium, which imposes resistance on the ejected material, leading to a deceleration effect. This phenomenon mirrors the behavior expected during the adiabatic (Sedov-Taylor) phase of the explosion, where in the expansion of the shock front is influenced by the surrounding medium's density.

Overall, the velocity profile of the ejected material exhibits distinct phases, each reflective of underlying physical processes governing the evolution of the supernova explosion. This nuanced understanding provides valuable insights into the dynamic interplay between the supernova remnant and its surrounding environment, shedding light on the complex dynamics of astrophysical phenomena.

2.4. Phase 3. Momentum Conserving Phase

In the progression of supernova remnants, the momentum-conserving phase emerges when the shock velocity diminishes to approximately match the sound speed of the surrounding gas. At this crucial juncture, significant transformations occur, including the fragmentation of the expanding shell and its assimilation into the interstellar medium.

Throughout this phase, the remnant undergoes a shift towards a momentum-conserving snow-plow stage. Here, its expansion adheres to a scaling law where the radius varies with the fourth root of the elapsed time, underscoring the intricate interplay between the remnant and its ambient environment. This phase assumes a pivotal role in shaping the enduring evolution of supernova remnants, influencing their interaction with the interstellar medium and their impact on galactic dynamics (Cioffi et al. 1988).

During the momentum-conserving phase, the remnant's expansion rate decreases as it gradually transfers momentum to the surrounding ISM. This transition from energy-dominated to momentum-dominated behaviour is crucial for shaping the remnant's long-term evolution. As the shock wave continues to interact with the ambient medium, it decelerates further, eventually merging with the surrounding ISM.

The scaling behaviour observed during the momentum-conserving phase, typically expressed as $R \propto t^{1/4}$, reflects the gradual deceleration of the shock wave's expansion. This power-law relationship indicates that the remnant's

radius increases more slowly over time compared to the initial energy-dominated phase.

3. Fermi Bubbles

In 2020, the X-ray telescope eRosita took images of two enormous bubbles extending far above and below the center of our galaxy (Predehl et al. 2020).
Two contrasting theories propose distinct mechanisms behind the formation of these colossal galaxy-sized bubbles. One theory suggests their emergence occurred when the supermassive black hole at the heart of the Milky Way devoured a substantial amount of matter, subsequently emitting a powerful beam of particles and radiation. In contrast, another theory argues that the bubbles resulted from the outflowing material propelled by an intense phase of star formation within our galactic center (Mann 2023). Additionally, hybrid models have been proposed, blending elements from both processes to account for the observed data.

These outflows from black holes originate as material approaches the black hole but does not pass beyond its event horizon—the boundary beyond which nothing can escape due to gravitational pull. As a result, some of this material is ejected back into space, preventing the uncontrolled growth of black holes. However, the energy expelled from the black hole displaces nearby material, leading to the formation of expansive bubbles in the surrounding space (Sherburne 2022).

The structures stand at a towering height of 11 kiloparsecs. For context, one parsec translates to approximately 3.26 light-years, equivalent to the distance light travels in a year, thrice over. Hence, these structures soar to an impressive altitude of nearly 36,000 light-years (Sherburne 2022).

3.1. Star Formation in the Galactic Center

In the Galactic center, star formation serves as a fundamental mechanism for providing the energy and material necessary to elucidate the gamma-ray emissions associated with the Fermi Bubbles phenomenon. The star formation processes occurring within this region are characterized by exceptionally protracted timescales and heightened areal density. Over the course of these extended periods, stars are continuously born and evolve, releasing energy through various processes such as nuclear fusion and stellar winds.

During the star formation process, relic cosmic ray protons and heavier ions are generated as byproducts (Owen et al. 2023). These cosmic rays are high-energy particles that possess significant kinetic energy. As they interact with the surrounding environment, including the interstellar medium and magnetic fields, they undergo acceleration processes that boost their energies even further.

In the context of the Fermi Bubbles, the relic cosmic ray protons and heavier ions injected into the surrounding space by the ongoing star formation in the Galactic center play a crucial role. These energetic particles contribute to the overall gamma-ray emission observed within the Fermi Bubbles. Their interactions with the surrounding gas, magnetic fields, and other cosmic structures produce gamma rays, which are detected and studied by observatories such as the Fermi Gamma-ray Space Telescope (Crocker and Aharonian 2011).

3.2. Structure of Fermi Bubbles

Two expansive, bubble-like formations have been identified by Su and others. (2010), Dobler et al. (2010), and Su and Finkbeiner (2012) in Fermi-*LAT* gamma-ray data, stretching approximately 50° above and below the Galactic center.

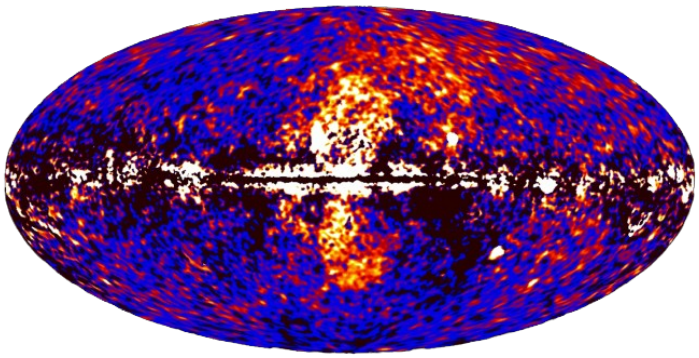

Fig. 16: Fermi-*LAT* Data Visualisation Showing Twoγ-ray Emitting Bubbles Emerging from Center of The Galactic Plane. (Credits: NASA/DOE/Fermi LAT/Finkbeiner (2004))

These structures, referred to as "Fermi bubbles" (FBs), display an E-2 type spectrum (Hooper and Slatyer 2013), markedly harder than the spectrum of the diffuse gamma-ray emission from the Galactic disk. Notably, features coinciding with or resembling the FBs have been observed at other wavelengths, including the microwave haze detected by the Wilkinson Microwave Anisotropy Probe (WMAP) (Finkbeiner 2004) and, more recently, in Planck data (Ade et al. 2013).
The large-scale biconical structure is believed to form due to mass ejections originating from the Galactic Center, spanning from small-scale arcminutes to larger scales of tens of degrees (Bland-Hawthorn and Cohen 2003).

These ejections are characterized by vigorous mass outflows from the Galactic Center, likely originating from either young star clusters or the central black hole, with estimated ages ranging between 5 million to 20 million years. Historical starburst events have been observed in the Galactic Center at various intervals, supported by detailed analyses of features and a comprehensive inventory of individual stars (Bland-Hawthorn and Cohen 2003).

3.3. Modelling Fermi Bubbles

To initiate the modelling of Fermi bubbles, we can draw upon established models and solutions devised for supernova explosions, albeit with tailored adjustments to specific parameters and underlying assumptions.

Primarily, it is conjectured that the density within Fermi bubbles exhibits non-linear variations over time, indicative of a nuanced evolution of these structures. This entails representing density as a function of radius, capturing its temporal fluctuations alongside other steadfast parameters such as interstellar medium density and the initial radius of the bubble. Such a characterisation enables a more comprehensive understanding of the dynamic interplay between various factors governing the evolution of Fermi bubbles
Additionally, it is assumed that the dense accreted material of the supermassive black hole (SMBH) within the Fermi bubble is distributed spherically across the bubble.

Hence, the equation used to describe the density profile of the Fermi bubble is:

$$\rho = \rho_0 \left(\frac{R_0}{R}\right)^2 \tag{12}$$

Integrating this equation over all space in a spherically symmetric area gives mass of the bubble

$$M = \int_0^R \rho(R') 4\pi R'^2 dR' \tag{13}$$

which gives the mass as

$$M = \rho_0 R_0^2 4\pi R \tag{14}$$

Equation 15 can be rearranged to find the radius as a function of mass and density which can then be modelled.

$$R = \frac{M}{4\pi\rho_0 R_0^2} \tag{15}$$

3.3.1. Insights from Supernovae Models

Various observations conducted over the years contribute to supporting different theories. For example, faint structures resembling a vestigial imprint of an AGN-like jet originating from the galactic center have been identified by several research teams. However, the data remains too faint to conclusively verify the AGN hypothesis(Cecil et al. 2021).

Advocates of the supernova wind theory highlight chimney-like formations observed in X-rays. These structures, extending several hundred light years in height and width from the galactic center, appear to be releasing energetic particles into the Fermi bubbles. The significant width of these chimneys suggests that they are not formed by a single point source such as the Milky Way's black hole but likely originate from star formation activity near the galactic center(Ponti et al. 2019).

3.3.2. Sedov-Taylor Solution for Fermi Bubbles

Drawing parallels with the intricate dynamics observed in supernova explosions, the Sedov-Taylor model emerges as a promising framework for simulating the expansion of Fermi Bubbles. However, distinguishing itself from conventional supernova modelling, the energy profile of Fermi Bubbles undergoes significant variations owing to the evolving optical characteristics intrinsic to the bubbles.
Embracing the notion that the energy content of Fermi Bubbles is inherently linked to their kinetic luminosity, dynamically radiating as time progresses ($E = L_{kin}t$)

Therefore, we encounter a nuanced depiction of momentum evolution:

$$\frac{d(4\pi\rho_0 R_0^2 R\dot{R})}{dt} = \frac{2E}{R} = \frac{2L_{kin}t}{R} \tag{16}$$

In consonance with the Sedov-Taylor methodology applied to supernovae 16, envisaged in the form of the form $R = At^\eta$
Therefore, solving the ordinary differential equation (see derivation 5), the solutions obtained are:

$$\eta = 1 \text{ and } A = \left(\frac{L_{kin}}{2\pi\rho_0 R_0^2}\right)^{\frac{1}{3}}$$

Therefore, the equation for the radius to be modelled can be written as

$$R = At = \left(\frac{L_{kin}}{2\pi\rho_0 R_0^2}\right)^{\frac{1}{3}} t \tag{17}$$

Delving deeper into the intricacies of Fermi Bubbles, we find their kinetic luminosity to be notably lower than the Eddington luminosity associated with Sgr A*. This distinction arises from their injection rate, which remains substantial at 10^{41} erg/s i.e. two orders of magnitude larger than the X-ray luminosity of a nebulae near the galactic center. Despite this significant injection rate, the kinetic luminosity of Fermi Bubbles modestly resides within the $5 - 10\%$ range of Sgr A*'s Eddington luminosity due to bubble being optically thin letting the luminosity i.e. the photon energy per second out of the bubble (Ryu et al. 2013).

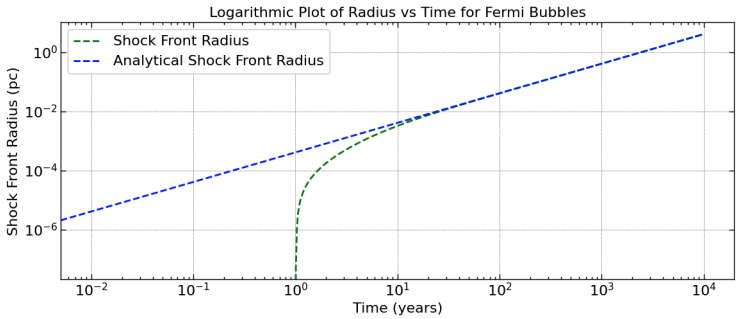

Fig. 17: Sedov-Taylor Solution for Fermi Bubbles

From the Figure 17, the plotted graph showcases the evolution of the shock front radius of Fermi bubbles over

time, providing insights into their expansion dynamics. As time progresses, the shock front radius, representing the outer boundary of the expanding bubble, exhibits a characteristic behaviour. Initially, during the early stages of expansion, the radius increases gradually, reflecting the gradual outward propagation of the shock wave.

3.3.3. Energy Visualisation for Fermi Bubbles

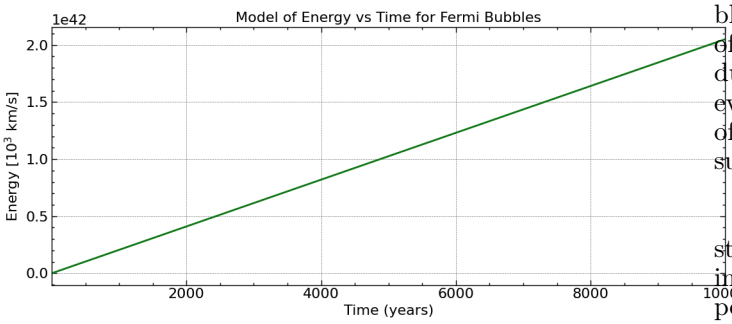

Fig. 18: Energy vs Time Graph for Fermi Bubbles

Visualising this as a logarithmic plot tells us that the energy of the Fermi Bubble although less due to the shell being optically thin and letting the photons escape, increases gradually over time.

This suggests a sustained source of energy fuelling the expansion and development of Fermi Bubbles. This phenomenon could be attributed to ongoing processes such as accretion onto Sagittarius A* (Sgr A*) or continuous feedback mechanisms stemming from star formation activities in the Galactic Center. As stars draw near the black hole, they encounter tidal forces that cause their disruption, resulting in the release of substantial energy in the form of radiation, stellar winds, and potentially relativistic jets (Ghez et al. 2008; Genzel et al. 2010).

4. Conclusion

Drawing from the insights gleaned from the cited literature, our paper embarks on a journey into the intricate dynamics of supernova remnants, Fermi Bubbles, and the enigmatic supermassive black hole residing at the heart of the Milky Way Galaxy. Our investigation delves deep into the evolutionary phases of supernova remnants, particularly focusing on the momentum-conserving snow-plow stage, where the remnant's expansion gradually relinquishes its energy dominance in favour of momentum transfer to the surrounding interstellar medium. This pivotal transition shapes the long-term evolution of supernova remnants, characterized by the scaling behaviour denoted by$R \propto t^{1/4}$, indicating the gradual deceleration of the shock wave's expansion over time.

Moreover, our research delves into the physical mechanisms underlying the formation of Fermi Bubbles, colossal structures extending above and below the Galactic center. We explore contrasting theories and propose that star formation processes in the Galactic center play a fundamental role in fuelling the energy and material necessary for the observed gamma-ray emissions associated with Fermi Bubbles. The extended periods of star formation in this region give rise to relic cosmic ray particles, which, upon interaction with the interstellar medium and magnetic fields, undergo acceleration processes, thereby enhancing their energies.

Additionally, our study sheds light on the activity of Sgr A*, the supermassive black hole at the Milky Way's center. We uncover past outbursts and interactions with molecular clouds, hinting at historical luminosity variations of the black hole over the past few decades. Notably, the detection of an X-ray echo emitted approximately two centuries ago during a period of heightened activity provides compelling evidence of Sgr A*'s dynamic behaviour, with the intensity of the X-ray emission during that epoch estimated to surpass current emissions.

In essence, our research contributes to a deeper understanding of the intricate astrophysical phenomena unfolding within our galaxy. By unravelling the dynamics of supernova remnants, Fermi Bubbles, and the activity of Sgr A*, we gain valuable insights into the underlying processes shaping galactic evolution and dynamics.

5. Appendix

5.1. Sedov-Taylor Solution Derivation for Supernovae Explosion

The ordinary differential equation required to derive the Sedov-Taylor can be written as

$$\frac{d\Pi_{SW}}{dt} = 4\pi R_{SW}^2 \times \frac{2}{3}\frac{E_{SN}}{V} \tag{18}$$

$$\frac{d}{dt}\left(\frac{4\pi}{3}\rho_0 R_{SW}^3 \dot{R}_{SW}\right) = 4\pi\ R_{SW}^2 \times \frac{2}{3}\frac{E_{SN}}{\frac{4\pi}{3}R_{SW}^3} \tag{19}$$

Assuming a power-law solution for O.D.E 19 of the form $R_{SW} = At^{\eta}$. Taking first derivative of the assumed solution with respect to time i.e. $\dot{R}_{SW} = \eta A t^{(\eta-1)}$

Therefore, the radial bit in the momentum equation (see equation 19) can be written in terms of power-law solution:

$$R_{SW}^3 \dot{R}_{SW} = \eta A^4 t^{(4\eta-1)} \tag{20}$$

Solving equation 19 with solved parameters from equation 20, the further solution obtained is

$$\frac{4\pi}{3}\rho_0 \eta A^4 (4\eta-1) t^{(4\eta-2)} = \frac{1}{2\pi}\frac{E_{SN}}{A^3 t^3 \eta} \times 4\pi A^2 t^{2\eta} \tag{21}$$

Rearranging equation 21 to obtain the following equation

$$A^5 \eta (4\eta-1) t^{(5\eta-2)} = \frac{3E_{SN}}{2\pi\rho_0} \tag{22}$$

Equation 22 can only be correct if the power of the time is equal to zero i.e. $5\eta - 2 = 0$ This gives the power $\eta = 2/5$

Therefore, the equation is now written as

$$A^5 \frac{2}{5} \times \frac{3}{5} = \frac{3E_{SN}}{2\pi\rho_0} \tag{23}$$

Re-arranging equation 23 to find A

$$A = \left(\frac{25E_{SN}}{4\pi\rho_0}\right)^{\frac{1}{5}} \tag{24}$$

5.2. Sedov-Taylor Solution Derivation for Fermi Bubble Expansion

The ordinary differential equation required to derive the Sedov-Taylor expression for Fermi Bubbles can be written as

$$\frac{d(4\pi\rho_0 R_0^2 R\dot{R})}{dt} = \frac{2E}{R} = \frac{2L_{kin}t}{R} \tag{25}$$

$$\frac{d\Pi}{dt} = \frac{2E}{R} = \frac{2L_{kin}t}{R} \tag{26}$$

Similar to supernovae model, assuming a power-law solution for O.D.E 25 of the form $R = At^{\eta}$. Taking first derivative of the assumed solution with respect to time i.e. $\dot{R} = \eta A t^{(\eta-1)}$

Therefore, the radial bit in the O.D.E. (see equation 25) can be written in terms of power-law solution:

$$\frac{d(4\pi\rho_0 R_0^2 A^2 \eta t^{(2\eta-1)})}{dt} = \frac{2L_{kin}t}{At^{\eta}} \tag{27}$$

Solving equation 27, the further solution obtained is

$$4\pi\rho_0 R_0^2 A^2 \eta (2\eta-1) t^{(2\eta-1)} = \frac{2L_{kin}t}{A} t^{(1-\eta)} \tag{28}$$

Equation 28 can only be correct if the power of the time constant on both side are equal to each other i.e. $2\eta - 1 = 1 - \eta$ Therefore, the obtained power is $\eta = 1$

Rearranging equation 28 with obtained power in 5 to obtain the following equation

$$4\pi\rho_0^2 A^3 = 2L_{kin} \tag{29}$$

Re-arranging equation 29 to find A

$$A = \left(\frac{L_{kin}}{2\pi\rho_0 R_0^2}\right)^{\frac{1}{3}} \tag{30}$$

References

Ade, P. A. R. et al. (2013), 'Planckintermediate results: Ix. detection of the galactic haze with planck', *Astronomy amp; Astrophysics* **554**, A139.
URL: *http://dx.doi.org/10.1051/0004-6361/201220271*

Bland-Hawthorn, J. and Cohen, M. (2003), 'The large-scale bipolar wind in the galactic center', *The Astrophysical Journal* **582**(1), 246–256.
URL: *http://dx.doi.org/10.1086/344573*

Borkowski, K. J. et al. (2001), 'Supernova remnants in the sedov expansion phase: Thermal x-ray emission', *The Astrophysical Journal* **548**(2), 820–835.
URL: *http://dx.doi.org/10.1086/319011*

Cecil, G., Wagner, A. Y., Bland-Hawthorn, J., Bicknell, G. V. and Mukherjee, D. (2021), 'Tracing the milky way's vestigial nuclear jet', *The Astrophysical Journal* **922**(2), 254.

Chiad, B. T., et al. (2015), 'Determination of velocity and radius of supernova remnant after 1000 yrs of explosion', *Int. J. Astron. Astrophys.* **05**(02), 125–132.

Cioffi, D. F., McKee, C. F. and Bertschinger, E. (1988), 'Dynamics of Radiative Supernova Remnants', *ApJ* **334**, 252.

Cramphorn, C. K. and Sunyaev, R. A. (2002), 'Interstellar gas in the galaxy and the x-ray luminosity of sgr a*in the recent past', *Astronomy I&; Astrophysics* **389**(1), 252–270.
URL: *http://dx.doi.org/10.1051/0004-6361:20020521*

Crocker, R. M. and Aharonian, F. (2011), 'Fermi bubbles: Giant, multibillion-year-old reservoirs of galactic center cosmic rays', *Physical Review Letters* **106**(10).
URL: *http://dx.doi.org/10.1103/PhysRevLett.106.101102*

Dobler, G., Finkbeiner, D. P., Cholis, I., Slatyer, T. and Weiner, N. (2010), 'Thefermihaze: A gamma-ray counterpart to the microwave haze', *The Astrophysical Journal* **717**(2), 825–842.
URL: *http://dx.doi.org/10.1088/0004-637X/717/2/825*

Díaz, J. S. (2021), 'Explosion analysis from images: Trinity and beirut*', *European Journal of Physics* **42**(3), 035803.
URL: *http://dx.doi.org/10.1088/1361-6404/abe131*

Finkbeiner, D. P. (2004), 'Microwave interstellar medium emission observed by thewilkinson microwave anisotropy probe', *The Astrophysical Journal* **614**(1), 186–193.
URL: *http://dx.doi.org/10.1086/423482*

Genzel, R. et al. (2010), 'The galactic center massive black hole and nuclear star cluster', *Reviews of Modern Physics* **82**(4), 3121–3195.
URL: *http://dx.doi.org/10.1103/RevModPhys.82.3121*

Ghez, A. M. et al. (2008), 'Measuring distance and properties of the milky way's central supermassive black hole with stellar orbits', *The Astrophysical Journal* **689**(2), 1044–1062.
URL: *http://dx.doi.org/10.1086/592738*

Gillessen, S. et al. (2009), 'Monitoring stellar orbits around the massive black hole in the galactic center', *The Astrophysical Journal* **692**(2), 1075–1109.
URL: *http://dx.doi.org/10.1088/0004-637X/692/2/1075*

Hooper, D. and Slatyer, T. R. (2013), 'Two emission mechanisms in the fermi bubbles: A possible signal of annihilating dark matter', *Physics of the Dark Universe* **2**(3), 118–138.
URL: *https://www.sciencedirect.com/science/article/pii/S2212686413000216*

Mack, J. and Ellis, U. S. (1946), 'Semi-popular motion-picture record of the trinity explosion', *Atomic Energy Commission* .

Mann, A. (2023), '"fermi" bubbles are bursting from our galaxy. their origins remain a mystery', *Proceedings of the National Academy of Sciences* **120**(47), e2318720120.
URL: *https://www.pnas.org/doi/abs/10.1073/pnas.2318720120*

Marin, F. et al. (2023), 'X-ray polarization evidence for a 200-year-old flare of sgr a*', *Nature* .
URL: *http://dx.doi.org/10.1038/s41586-023-06064-x*

Mathis, J. S. (2024), 'Supernova remnant'.
URL: *https://www.britannica.com/science/supernova-remnant*

Nayakshin, S. and Zubovas, K. (2018), 'Sgr a* envelope explosion and the young stars in the centre of the milky way', *Monthly Notices of the Royal Astronomical Society: Letters* **478**(1), L127–L131.
URL: *http://dx.doi.org/10.1093/mnrasl/sly082*

Owen, E. R., Wu, K., Inoue, Y., Yang, H. Y. K. and Mitchell, A. M. W. (2023), 'Cosmic ray processes in galactic ecosystems'.

Ponti, G., Hofmann, F., Churazov, E., Morris, M., Haberl, F., Nandra, K., Terrier, R., Clavel, M. and Goldwurm, A. (2019), 'An x-ray chimney extending hundreds of parsecs above and below the galactic centre', *Nature* **567**(7748), 347–350.

Ponti, G. et al. (2010), 'Discovery of a superluminal fe k echo at the galactic center: The glorious past of sgr a* preserved by molecular clouds', *The Astrophysical Journal* **714**(1), 732–747.
URL: *http://dx.doi.org/10.1088/0004-637X/714/1/732*

Predehl, P. et al. (2020), 'Detection of large-scale x-ray bubbles in the milky way halo', *Nature* **588**(7837), 227–231.

Ryu, S. G., Nobukawa, M., Nakashima, S., Tsuru, T. G., Koyama, K. and Uchiyama, H. (2013), 'X-ray echo from the sagittarius c complex and 500-year activity history of sagittarius a*', *Publications of the Astronomical Society of Japan* **65**(2).
URL: *http://dx.doi.org/10.1093/pasj/65.2.33*

Sherburne, M. (2022), 'Massive bubbles at center of milky way caused by supermassive black hole', `https://news.umich.edu/massive-bubbles-at-center-of-milky-way-caused-by-supermassive-blac` Accessed: 2024-4-6.

Su, M. and Finkbeiner, D. P. (2012), 'Evidence for gamma-ray jets in the milky way', *The Astrophysical Journal* **753**(1), 61.
URL: *http://dx.doi.org/10.1088/0004-637X/753/1/61*

Su, M. and others. (2010), 'Giant gamma-ray bubbles fromfermi-lat: Active galactic nucleus activity or bipolar galactic wind?', *The Astrophysical Journal* **724**(2), 1044–1082.
URL: *http://dx.doi.org/10.1088/0004-637X/724/2/1044*